

Solid state based analog of optomechanics

Nicolas L. Naumann,¹ Leon Droenner,¹ Alexander Carmele,¹

Andreas Knorr,¹ Weng W. Chow,² and Julia Kabuss¹

¹*Institut für Theoretische Physik, Nichtlineare Optik und Quantenelektronik,
Technische Universität Berlin, Hardenbergstr. 36, 10623 Berlin, Germany*

²*Sandia National Laboratories, Albuquerque, New Mexico 87185-1086, USA*

Abstract

We investigate a semiconductor quantum dot as a microscopic analog of a basic optomechanical setup. We show, that optomechanical features can be reproduced by the solid-state platform, arising from parallels of the underlying interaction processes, which in the optomechanical case is the radiation pressure coupling and in the semiconductor case the electron-phonon coupling. In optomechanics, phonons are typically induced via confined photons, acting on a movable mirror, while in the semiconductor system the phonons are emitted by the laser-driven electronic system. There are analogous effects present for both systems, featuring bistabilities, optically induced phonon lasing and enhanced phonon loss. Nonetheless, the different statistical nature of the optical cavity and the electronic system also leads to qualitative differences.

PACS numbers: 42.65.Sf,42.50.Wk,78.67.Hc,63.20.K-

Keywords: Optomechanics, semiconductor quantum dot, phonons, bistability

I. INTRODUCTION

Quantum optomechanics (OM) has been rapidly developing into a major research area over the last decades^{1,2}. Intense activities are fueled by interesting physics based on radiation pressure arising from momentum transfer between photons and optical surfaces. The phenomenon affects ultra-accurate measurements (e.g., gravitational wave detection³) and can lead to nanoscale motors and refrigerators⁴.

This manuscript proposes and analyzes a different physical system for exploring a semiconductor (SC) analog of quantum optomechanics. It differs from the atomic-molecular-optical (AMO) approach to optomechanics in that radiation pressure is replaced by the electron-phonon interaction. The presence of electron-phonon interaction usually leads to heating in optoelectronic devices⁵. However, if optically addressing phonon assisted resonances or when properly modifying and harnessing electron-photon interaction in an acoustic cavity, the same combination of interactions can be useful, e.g., provide high-temperature single-photon generation⁶, optoelectronic self-cooling and memory in silicon photonics. There is interesting physics as well, e.g. enabling of strong-coupling physics, via a quantum-mechanical polariton-polaron superposition^{7,8}.

Several proposals of phonon cavities coupling an acoustic phonon mode to the electronic degrees of freedom have been made^{9,10} and even though there are challenges such as anharmonic phonon decay or fluctuations in layer thickness, high-Q phonon cavities have been realized experimentally¹¹⁻¹⁴. Besides such a designed electron-acoustic phonon coupling, that enables the interaction with a selected acoustic phonon mode, many semiconductor nanostructures naturally inherit a strong effective single mode electron-phonon coupling mechanism, i.e. the coupling to longitudinal optical (LO) phonons^{15,16}. At optical excitation, these systems may find applications as phonon lasers¹⁷.

A possibility of these new applications and physical effects comes from the semiconductor electron-phonon coupling mechanism being stronger than radiation pressure. Further, the solid state platform typically involves much larger phonon frequencies^{1,17}, especially in the case of LO phonons. This in particular enables a controlled selection of subsystems for effective phonon lasing or damping only by the choice of optical input frequencies. The sketch in Fig. 1(a) depicts the basic cavity quantum optomechanics setup. Photons give momentum to the cavity mirrors upon reflection, which then changes the mirror position and affects

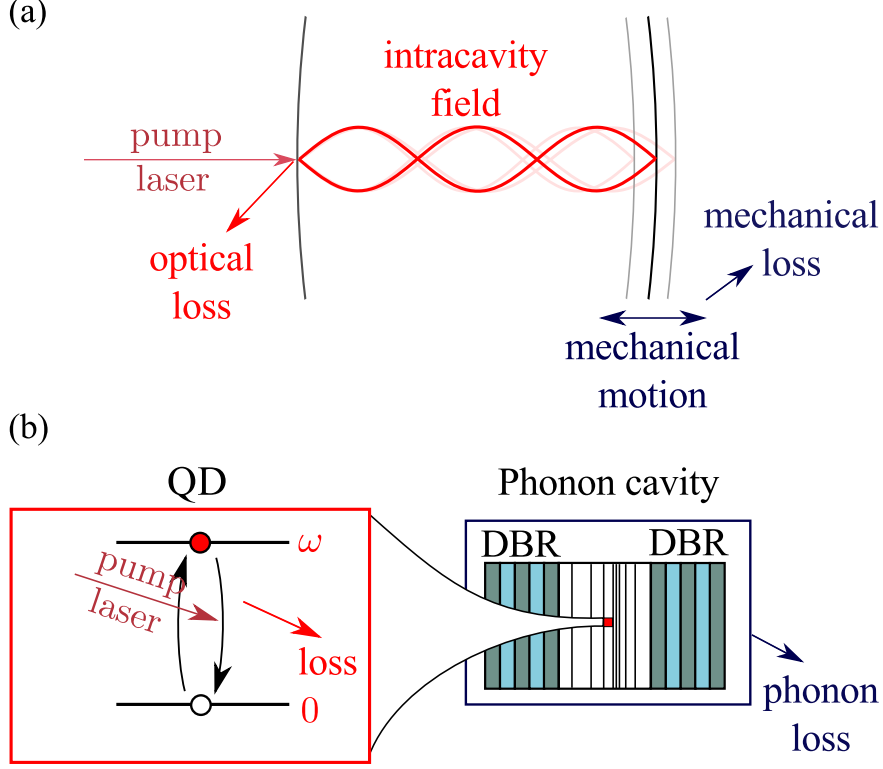


Figure 1. (a) Basic setup for investigating cavity quantum optomechanics. (b) Proposed semiconductor quantum optical approach to exploring acoustic phonon dynamics. The phonon cavity consists of materials of alternating acoustic impedance in analogy to an optical distributed Bragg reflectors (DBR)^{11,14}.

ultra-high precision (atomic scale) measurements. The Hamiltonian has the form¹

$$H_{\text{OM}} = \hbar\omega_{\text{cav}}\hat{c}^\dagger\hat{c} + \hbar\Omega_{\text{m}}\hat{b}^\dagger\hat{b} + i\hbar E_1 (\hat{c}^\dagger e^{-i\omega_L t} - \hat{c} e^{i\omega_L t}) - \frac{\hbar\omega_{\text{cav}}}{L} \sqrt{\frac{\hbar}{m\Omega_{\text{m}}}} \hat{c}^\dagger \hat{c} \frac{(\hat{b} + \hat{b}^\dagger)}{\sqrt{2}}. \quad (1)$$

Here, \hat{c} (\hat{c}^\dagger) is the cavity phonon annihilation (creation) operator and ω_{cav} the cavity frequency. Ω_{m} is the frequency of the mechanical oscillator and \hat{b} (\hat{b}^\dagger) the corresponding annihilation (creation) operator. The third term models the driving by an external laser and the last term is the coupling due to radiation pressure, where L is the length of the cavity, m the mass of the mirror.

The sketch in Fig. 1(b) is our proposed alternate experimental configuration for the semi-

conductor system, with the Hamiltonian

$$\begin{aligned}
H_{\text{SC}} = & \hbar\omega_v \hat{a}_v^\dagger \hat{a}_v + \hbar\omega_c \hat{a}_c^\dagger \hat{a}_c \\
& + i\hbar E_1 (\hat{a}_c^\dagger \hat{a}_v e^{-i\omega_L t} - \hat{a}_v^\dagger \hat{a}_c e^{i\omega_L t}) \\
& + \hbar \sum_{\mathbf{q}} \omega_{\mathbf{q}} \hat{b}_{\mathbf{q}}^\dagger \hat{b}_{\mathbf{q}} + (g_{\mathbf{q}}^c - g_{\mathbf{q}}^v) \hat{a}_c^\dagger \hat{a}_c \hat{b}_{\mathbf{q}} + H.c. \quad (2)
\end{aligned}$$

Here, \hat{a}_v or \hat{a}_c (\hat{a}_v^\dagger or \hat{a}_c^\dagger) are the annihilation (creation) operators of an electron in the valance band or conduction band, respectively. In this case, $\hat{b}_{\mathbf{q}}$ ($\hat{b}_{\mathbf{q}}^\dagger$) is the annihilation (creation) of a phonon with the frequency $\omega_{\mathbf{q}}$. In this case, the electronic transition is driven optically. Furthermore, the phonon modes will be treated as one effective phonon mode.^{15,16}

We want to emphasize some formal similarities of the Hamiltonians: In place of the photon number operator in the AMO case, there is the electron population operator. In conventional quantum optomechanics, the photons create or remove mirror motion. In our case [Eq.(2)], a laser-driven electronic transition creates or annihilates a phonon. The coupling constants are of course different.

The Hamiltonians for both systems can be brought to the form of Eq. (3), where we included additional electronic transitions, which are excited optically, for additional quantum dots. We now introduce a common nomenclature for the elements of both systems for notational convenience and to emphasize the similar roles the components play for the effects studied below. Thus, in the optomechanical system the photon mode is of high frequency (HF), while in the semiconductor system a two level system, which models a quantum dot, constitutes the HF part. The low frequency (LF) component is the mechanical mode of the oscillating mirror in the optomechanical case, whereas in the semiconductor case the phonon mode inside an acoustic cavity, as discussed before, is the LF part.

From the sketches [cf. Fig. 1], it may seem like the semiconductor version is more complicated than the AMO one. However, with the actual experimental setups, the exact opposite is true. Conventional quantum optomechanics can involve large and complicated setups, like the LIGO for detecting gravitational wave. But there are also microscopic optomechanical devices, which maximize the optomechanical coupling strength by small oscillator masses. To do this, a broad range of designs exists in addition to the classical Fabry-Perot-Setup, using e.g. whispering gallery modes or photonic crystals¹.

The semiconductor system is on a chip, and very much like a photonic integrated circuit with the possibility of incoherent pumping of the semiconductor active medium. From the

AMO side, connecting the two approaches increases enormously the relevance of quantum optomechanics, because of the widespread use of optoelectronic devices. For example basic quantum mechanical features, such as the formation of mechanical polarons in polariton optomechanics⁷ as optomechanical counterpart to the polaron formation in typical semiconductor cavity quantum electrodynamics can be expected in quantum hybrid systems. From the semiconductor side, making the connection to AMO quantum optomechanics gives guidance on what may be interesting or useful to explore, transferring predictions and techniques for optomechanics devices onto optoelectronic platforms.

With this guidance, we developed an analogy between the optomechanical coupling and semiconductor quantum-dot system and choose as demonstration of similarity between the two approaches three exemplary effects, which can be found in both cases. The manuscript is structured as follows. In Sec. II, we introduce the Hamiltonian, which can be brought to the same form for both systems. The first effect we consider in Sec. III is the bistability as a prototypical nonlinear effect. Next, mechanical lasing, also known as phonon lasing, is discussed in Sec. IV. It is present in optomechanical^{1,18,19} as well as in the semiconductor systems¹⁷. Finally, in Sec. V, the basis of laser cooling of mechanical motion will be discussed, which can be observed in optomechanical systems²⁰. Theoretically, it can be understood as an enhancement of the effective damping of the mechanical oscillator²¹. We compare the realization of these effects in the above systems.

II. COMPARISON

We compare two different physical systems to explore mutual effects but also to elaborate on differences. On the one hand, we are interested in an optomechanical system, which consists of an optically pumped cavity mode, which is coupled by radiation pressure to a mechanically oscillating mirror. As a semiconductor counterpart of such an optomechanical setup we investigate optically pumped quantum dots (QDs), that are coupled to a single phonon mode.

The second case may be realized in two ways: The phonon mode is either a single confined acoustic phonon mode or an effective mode describing the collective motion of several optical phonon modes.

Both systems can be described by very similar sets of equations of motion, which will be

shown in the following. Thus, even though the main difference is the statistics of the HF mode, some differences will only arise from the choice of parameters.

Despite all of the above mentioned effects being present in both, the OM and SC system, their origin is of different nature and thus also their experimental realization. As we will see in the following, the crucial difference between the systems is the behavior of the component, that is coupled to the mechanical degree of freedom. In the OM, the mechanical mode is coupled to an optical mode, which is bosonic and can thus have an arbitrary number of excitations. In the SC system, the phonon mode is coupled to one or several QDs, which constitute an electronic and thus a fermionic system.

In this manuscript the QDs are modeled as a number of two-level systems (TLS). Therefore, the SC system can only contain a limited number of excitations. But also in more complex electronic systems the number of excitations is in principle restricted, which is not the case for the optical cavity in the OM system. This will lead to some major differences between the systems. E.g. cycling processes, discussed in the context of lasing, can be affected more strongly by electronic lifetimes. However, we will show that within certain parameter regimes and a selection of quantities the SC system can approach the OM one for a large number of QDs. Then the possible number of excitations becomes very large, as in the OM case, which would strictly be the limit of an infinite number of QDs.

Hamiltonian — The basis of our analysis constitutes a Hamiltonian model. The Hamiltonians can be written in the same form for both systems^{17,22}

$$H = \hbar\Omega\hat{b}^\dagger\hat{b} + \hbar\omega\hat{\mathbf{p}}^\dagger\hat{\mathbf{p}} + \hbar g\hat{\mathbf{p}}^\dagger\hat{\mathbf{p}}\left(\hat{b} + \hat{b}^\dagger\right) + i\hbar\mathbf{E}\left(\hat{\mathbf{p}}^\dagger e^{-i\omega_L t} - \hat{\mathbf{p}} e^{i\omega_L t}\right). \quad (3)$$

The terms can be identified with the different components of each system: The first term is the mechanical or the phonon mode in the optomechanical and the semiconductor system, respectively. They are modeled as a single harmonic oscillator with frequency Ω . Then \hat{b} (\hat{b}^\dagger) is the annihilation (creation) operator for one phonon (we will also call the mechanical excitations of the oscillating mirror phonons), so the commutation relation reads $[\hat{b}, \hat{b}^\dagger] = 1$ in both cases. This constitutes the part of the system with low frequency (LF) in comparison to optical frequencies. The second term models the cavity mode or the QDs. As shorthand notation, we introduce the vector $\hat{\mathbf{p}}$ with elements \hat{p}_j , whose length depends on the system. In the OM system, there is only one element, namely the optical cavity, and thus $\hat{p}_1 = \hat{c}$.

The cavity is modeled as a harmonic oscillator oscillating at frequency ω . The annihilation (creation) operator for the cavity mode is \hat{c} (\hat{c}^\dagger) (it is also $[\hat{c}, \hat{c}^\dagger] = 1$). The commutation relations for the degrees of freedom of the QDs differ due to their fermionic nature. In this case, $\hat{\mathbf{p}}$ is now a vector with N_{QD} elements \hat{p}_j , where N_{QD} is the number of QDs coupled to the mechanical mode. In the following, we are interested in the case of N_{QD} identical QDs (inhomogeneous broadening is neglected).

We can now identify $\hat{p}_j = \hat{a}_{\mathbf{v},j}^\dagger \hat{a}_{\mathbf{c},j}$ ($\hat{p}_j^\dagger = \hat{a}_{\mathbf{c},j}^\dagger \hat{a}_{\mathbf{v},j}$), with the anti-commutation relations $\{\hat{a}_{\mu,j}, \hat{a}_{\nu,l}^\dagger\} = \delta_{\mu,\nu} \delta_{j,l}$. Here, the $\hat{a}_{\mu,j}$ ($\hat{a}_{\mu,j}^\dagger$) are the annihilation (creation) operator for an electron in the band μ of the j th QD mentioned in the introduction. of the j th QD. Here, we see that either the optical cavity or the QDs constitute the high frequency (HF) part of the respective system, since they oscillate at optical frequencies. The third term gives the coupling of the two elements with the coupling strength g . The number of excitations in the system $\hat{\mathbf{p}}^\dagger \hat{\mathbf{p}}$ is coupled to the position of the LF mode $q = (\hat{b} + \hat{b}^\dagger)/\sqrt{2}$. The last term is the pumping term, which describes the external pumping of the coherence $\hat{\mathbf{p}}$ by a classical field with frequency ω_L . Here, \mathbf{E} is again a vector and consists of the individual pump strengths E_j of the QDs.

Equations of motion — From the Hamiltonian (3) the equations of motion can be derived. For the expectation value of some operator \hat{O} they are given by

$$\begin{aligned} \frac{d}{dt} \langle \hat{O} \rangle &= \frac{i}{\hbar} \langle [H, \hat{O}] \rangle + \gamma \text{Tr}(\hat{O} \mathcal{L}[\hat{\mathbf{p}}] \rho) + \kappa \text{Tr}(\hat{O} \mathcal{L}[\hat{b}] \rho) \\ &\quad + \frac{\gamma_{\text{PD}}}{2} \text{Tr}(\hat{O} \mathcal{L}[\sigma_z] \rho), \\ \mathcal{L}[\hat{X}] \rho &= 2\hat{X} \rho \hat{X}^\dagger - \hat{X}^\dagger \hat{X} \rho - \rho \hat{X}^\dagger \hat{X}, \end{aligned} \quad (4)$$

where damping and pure dephasing are taken into account in the Lindblad form. In the OM system the cavity mode is radiatively damped with γ , which is caused by scattering to other modes, outcoupling and imperfections of the mirrors. The mirror is damped with κ because of relaxation to the environment. In the SC system the damping rate of the excited electronic state is given by 2γ and the damping rate of the phonon mode is κ . These originate from couplings to not explicitly treated photon and phonon bath modes. The pure dephasing exists only for the SC system with optical phonons.

From Eq. (4), a system of equations is derived. For simplicity, we assume coherent fields and factorize products of operators into products of expectations values. Finally, the excitation

of the QDs is assumed to be equal for all QDs and that they follow the same dynamics. Then, the dynamics of each QD is described by the same equations. In the OM case, there are two equations, while we need three for the description of the SC system. The additional equation occurs since, for the optical cavity system, the number of excitations can be factorized into the coherences: $\langle \hat{c}^\dagger \hat{c} \rangle = \langle \hat{c}^\dagger \rangle \langle \hat{c} \rangle$. In contrast, $\langle \sigma_{+,j} \sigma_{-,j} \rangle$ cannot be factorized, as this would imply that one individual QD can be excited more than once. After transforming the HF component to a frame rotating at the frequency of the external pump laser ω_L , the equations of motion read (shorthand notations for the expectation values: $P = \langle \hat{p}_1 \rangle e^{i\omega_L t}$, $B = \langle \hat{b} \rangle$, and, only for the SC system, $U = \langle \hat{p}_1^\dagger \hat{p}_1 \rangle$)

$$\dot{B} = -(i\Omega + \kappa)B - igNU \quad (5a)$$

$$\begin{aligned} \dot{P} &= (i\Delta - \gamma - \gamma_{PD})P - ig(B + B^*)P \\ &\quad + E_1(1 - U \mp U) \end{aligned} \quad (5b)$$

$$\dot{U} = E_1(P + P^*) - 2\gamma U. \quad (5c)$$

Here, the negative sign in Eq. (5b) is valid for the SC system, while the positive one holds for the OM system. Then, pump term does not depend on the occupation on the HF component, and Eq. (5c) becomes obsolete. Also, the occupation $U = P^*P$. In the SC case $N = N_{\text{QD}}$, while in the OM case $N = 1$, since only one cavity mode is considered.

The equations for the coherences P and B are formally identical: The HF component rotates at the frequency given by the detuning from the external pump laser $\Delta = \omega_L - \omega$ and is damped by γ . The coherence of the HF component is coupled to the position of the LF component, which effectively leads to a shifted frequency. Additionally, it is pumped by the external laser. In the OM system, the pumping term is not limited, while the pump in the SC system is restricted, since the QDs are saturated at some point. Finally, the coherence is coupled to the excitation of the HF component. The last equation describes the excitation of the upper level to account for the fermionic behavior in the SC system and contains a term with pumping and a term with damping.

As shorthand notation we define the expectation value for the number of excitations in the HF component as $n_{\text{HF}} = NU$, which becomes for the OM system $n_{\text{HF}} = P^*P$. In the OM system this is the number of cavity photons, while it is the number of electronic excitations in the SC system. The expectation value for the number of excitations in the LF component,

i.e. the phonon number, is defined as $n_{\text{LF}} = B^* B$. The OM equations are also valid for the SC system, when an individual quantum dot is excited marginally, which was shown in the context of spin systems, modeled by TLSs²³.

III. BISTABILITY

The first example we will give to show the similarities of the systems is the bistable behavior. The optomechanical bistability has been considered.²⁴ The equation for the steady state can be derived from (5) by setting the derivatives to zero. Furthermore, the stability of the steady state can be investigated by linearizing the system of equations in vicinity of the steady state²⁵. The bistability in the phonon number is given in Fig. 2(a) for the OM system and in Figs. 2(b) and 2(c) for the SC system with acoustic phonons and with optical phonons, respectively. In all cases a bistability can be observed. For understanding the origin of the bistability, we will have a closer look at the forces on the LF component, which are given by $F_{\text{tot}} = (\dot{B} - \dot{B}^*)/(\sqrt{2}i)$.

There are two competing forces acting on the LF component: The restoring force resulting from the harmonic potential F_h on the one hand and the force given by the coupling to the HF component F_c . In the steady state, an equilibrium of forces $F_{\text{tot}} = F_h + F_c = 0$ must prevail. When referring to a steady state value rather than the variable, we will add the index s . In the steady state, the restoring force is the same in both cases and linear with respect to the displacement $q_s = (B_s + B_s^*)/\sqrt{2}$ of the LF component

$$F_h = \left(\Omega + \frac{\kappa^2}{\Omega} \right) q_s. \quad (6)$$

In contrast to this the force F_c , originating from the coupling of the phonon mode to the electronic excitation, is a nonlinear function of the displacement of the LF component

$$F_{c,\text{SC}} = \frac{Ng}{\sqrt{2}} \frac{1}{1 + \frac{\gamma}{\gamma + \gamma_{\text{PD}}} \frac{(\Delta - \sqrt{2}gq_s)^2 + (\gamma + \gamma_{\text{PD}})^2}{2E_1^2}}. \quad (7)$$

The radiation pressure force in the OM case is obtained in the limit $N = 1$, $\gamma_{\text{PD}} = 0$ and $E_1^2 \ll (\Delta - \sqrt{2}gq_s)^2 + \gamma^2$ as

$$F_{c,\text{OM}} = \frac{g}{\sqrt{2}} \frac{2E_1^2}{(\Delta - \sqrt{2}gq_s)^2 + \gamma^2}. \quad (8)$$

Bistabilities

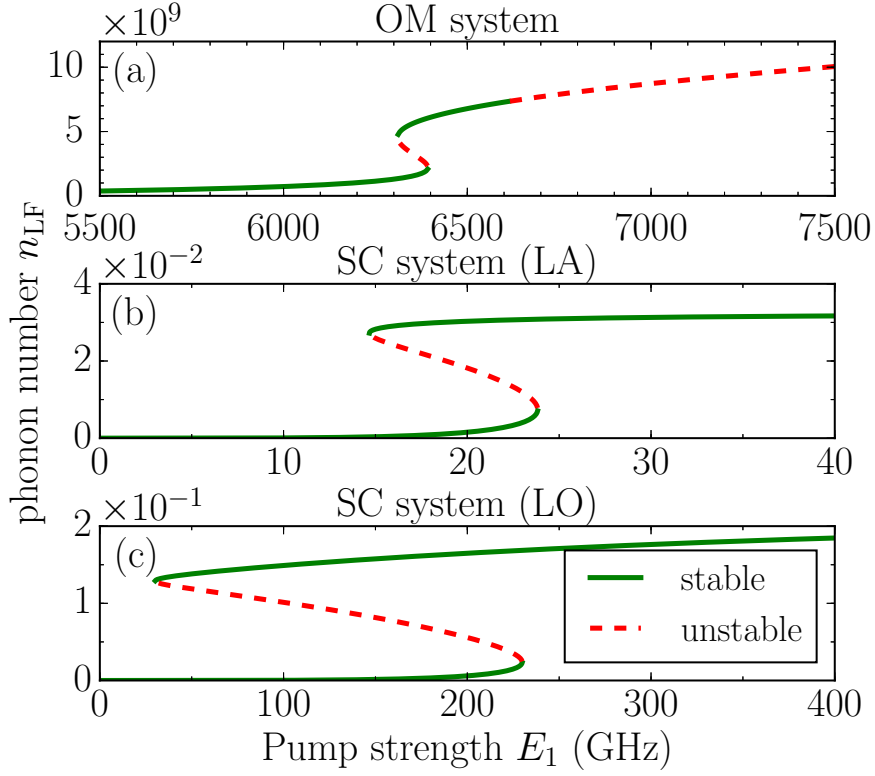


Figure 2. Stationary states of the phonon number n_{LF} for (a) the OM system, (b) the SC system with acoustic phonons, and (c) for the SC system with optical phonons. Note the difference in pump strength for bistability to occur. The parameters are given in Tab. I.

A bistability can only be observed, for detunings $\Delta < 0$, because there lies the maximum of F_c , regardless of the sign of g . Then, up to three equilibrium positions may occur.

The difference between the OM and the SC case originates from the fact, that the force acting on the phonon mode is affected by the number of excitations in the HF component. The radiation pressure force can be increased by increasing E_1 , even if the OM coupling constant is small. For the SC system, the absolute value of $F_{c,SC}$ is at maximum $\frac{Ng}{\sqrt{2}}$. Thus, either the coupling constant g has to be large enough, or the number of QDs has to be increased. Otherwise, pumping the QDs more strongly does not increase the force acting on the phonons, so that it may not become large enough to exhibit a bistability. This difference can be traced back to the statistics of the HF component, since its excitation can be increased arbitrarily by pumping in the OM case, while it is limited too in the fermionic

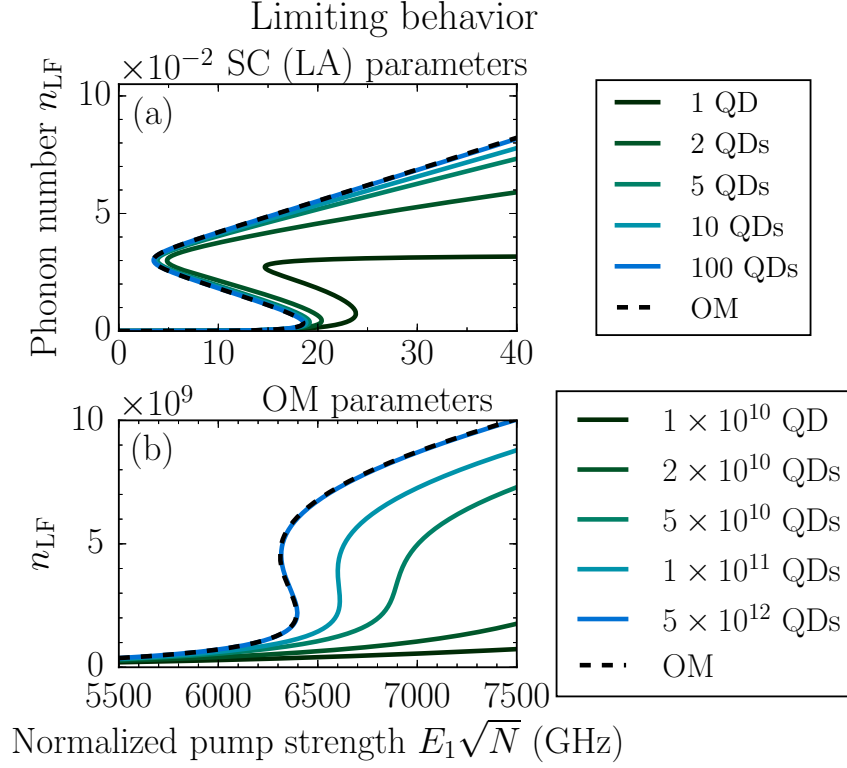


Figure 3. The limiting behavior of the stationary states of the phonon number n_{HF} for the SC system (a) with parameters for LA phonons and (b) with OM parameters. An increasing number of TLSs is shown: In the limit $N \rightarrow \infty$, the OM solution (dashed) is approached (parameters as in 2(b)).

case.

In App. A, we show that the equation for the SC system approaches the OM one for $N \rightarrow \infty$ and $\gamma_{PD} = 0$, when the pump strength is rescaled according to $E_1\sqrt{N_{QD}}$. This is illustrated for the SC system with LA phonons in Fig. 3(a). When the number of QDs is much larger than the typical number of phonons, the OM solution is reached by the SC system. In this case the coupling constant g is large enough, so that already for $N = 1$ a bistability can be observed.

The same transition is shown for OM parameters in Fig. 3(b). In this case there is only a bistability for a large number of TLS, since the coupling constant g is rather small. For both cases the ratio $N_{QD}/n_{LF} \approx 10^3$ gives an estimate for the number of QDs, for which the SC system coincides with the OM one. Here, n_{LF} is the stationary phonon number in the regime of the bistability.

With this, the major difference in Figs. 2 can be explained: In the OM case the phonon number is very high (in the order of 10^9), while it is rather low in the SC systems, since a bistability with a small coupling constant can only be observed, if the radiation pressure force is increased sufficiently through a high intensity in the optical cavity. In the SC systems, the bistability occurs already for very few phonons, since the electron-phonon coupling is stronger.

Note, that in the SC system with optical phonons also pure dephasing is taken into account. Then the system is in a regime, where for one QD no bistability can be observed, but ten QDs suffice to obtain a bistability [cf. Fig. 2(c)]. With the additional pure dephasing, the limiting behavior shown above is not valid.

After considering the bistability, which is a shared stationary property of the systems and motivates the OM system as a limiting case of the SC system with a large number of QDs, we will consider dynamical effects in the following sections.

IV. LASING

Fig. 3 suggests that the differences between the systems are more quantitative in nature. In the following, we will consider phonon lasing and damping. These processes, will reveal more profound differences between the two setups. At first, we will examine the effect known as mechanical or phonon lasing: A high number of coherent phonons is created in the mechanical mode. It has been investigated for the OM^{1,18,19} as well as for the SC system¹⁷. Here, we focus on the comparison of the two systems.

Induced phonon creation, that is exploited for phonon lasing can be understood as an anti-Stokes process of at least second order. For a most efficient build up of phonon population, the pump laser has to be blue detuned with respect to the HF resonance by roughly a multiple of the phonon frequency $n\Omega$. Due to a higher order energy conserving process, an excitation of the LF mode is achieved, when exciting the HF component [cf. Fig. 4]. At this point a major difference between the OM and the SC system already becomes apparent: For the OM system the upper- and the lower level in Fig. 4 may represent two arbitrary photon number states with $n - 1$ and n photons. Thus, the process is not restricted by the cavity decay rate κ . However, for the SC system, the excitation process can only occur, if the QD is decayed into its ground state. Therefore, the possibility of creating a phonon within this

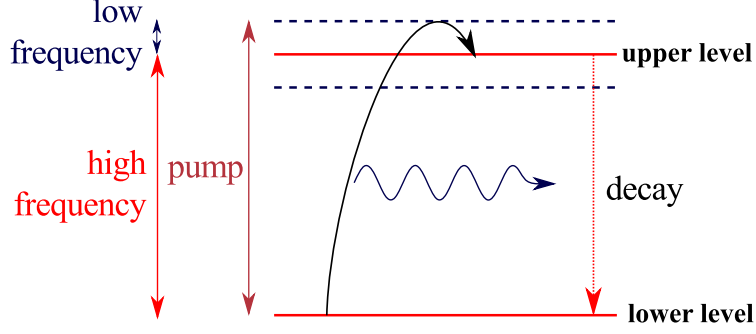


Figure 4. Scheme of the mechanism leading to lasing. See text for explanation.

anti-Stokes process is limited by the decay time of the QD excitation.

In the semiclassical model phonon lasing manifests itself as a parametrical instability: The steady state of low phonon number [cf. Sec. III] becomes unstable and the system reaches a periodic orbit of high phonon number. This is shown in Fig. 5 for the OM system and the SC system with LA and LO phonons. For the OM and the SC system with LA phonons the amplitude of the oscillations is small in comparison to the number of phonons since the damping of the phonon mode is rather small [See tab. II]. This way, new phonons are generated via the above described process, while phononic excitation is still present. However, in the SC system with LO phonons, the phonon lifetimes are typically very small, while the radiative lifetime of the QD excitations remains the same. The creation of LO-phonons, in particular coherent phonons is therefore not as efficient [Fig. 4] and the phononic excitation decays for the most part before a new phonon is created.

In Figs. 6 we show the mean phonon number in the system as a function of the detuning and the pump strength for the different systems. In case of the SC system, the number of QDs is further illustrated to have a crucial impact on the phonon lasing properties, such as thresholds or maximally achieved phonon number. For the OM system, we observe a maximum of the mean phonon number at the phonon assisted resonance for lower pump strengths [cf. Figs. 6(a)]. Pumping more strongly involves higher order processes, leading to a maximum at higher detunings. For the SC system, we note first of all, that the maximum phonon number is roughly proportional to the number of QDs [cf. Figs. 6(b)-(d)], which is consistent with the fact, that the QD excitations have to decay before the generation of a phonon can take place, i.e. in order to realize a phonon laser cycle. The next aspect, that can be observed, is that the maxima for phonon lasing are at the polaron-shifted phonon

Lasing: Time evolution

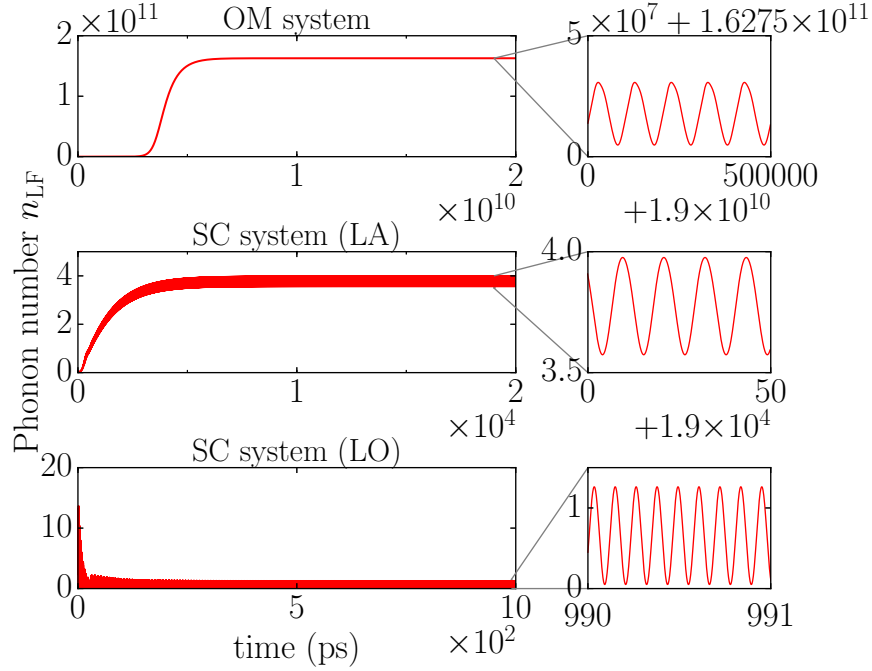


Figure 5. The time evolution for exemplary parameters [cf. Tab. II] is shown for the OM (a), the SC system with LA phonons (b), and for the SC system with LO phonons.

assisted resonances for lower pump strengths: In the case of a single QD $N = 1$, only the first phonon-assisted resonance involving the first order anti-Stokes process (as depicted in Fig. 4) contributes to phonon lasing. For a larger number N of QDs [cf. Figs. 6(c),(d)] also the resonance involving two phonons becomes visible. In relation to this, we observe a shift of the resonance-condition for phonon-lasing. This can be evaluated approximately by considering an effective system accounting for the second order process depicted above. This is shown in App. B, which follows Ref.¹⁷. The detuning from the effective QD resonance can be approximated as $\Delta_{\text{eff}} = -\Delta - 2\frac{E_1^2}{\Delta} - n_{\text{HF}}\frac{g^2}{\Omega}$. The resonance given by the detuning (first term), as defined in II, is altered by self-quenching (second term) with the pump strength and by the polaron shift (third term) with the electron-phonon coupling strength. For more than one QD [cf. Figs. 6(c),(d)] the polaron shift is proportional to the number of QDs. However, the QD excitation saturates fast, so that the shift is approximately constant in the lasing regime. The characteristic shift with the pump strength originates in the case of the SC system from the self quenching.

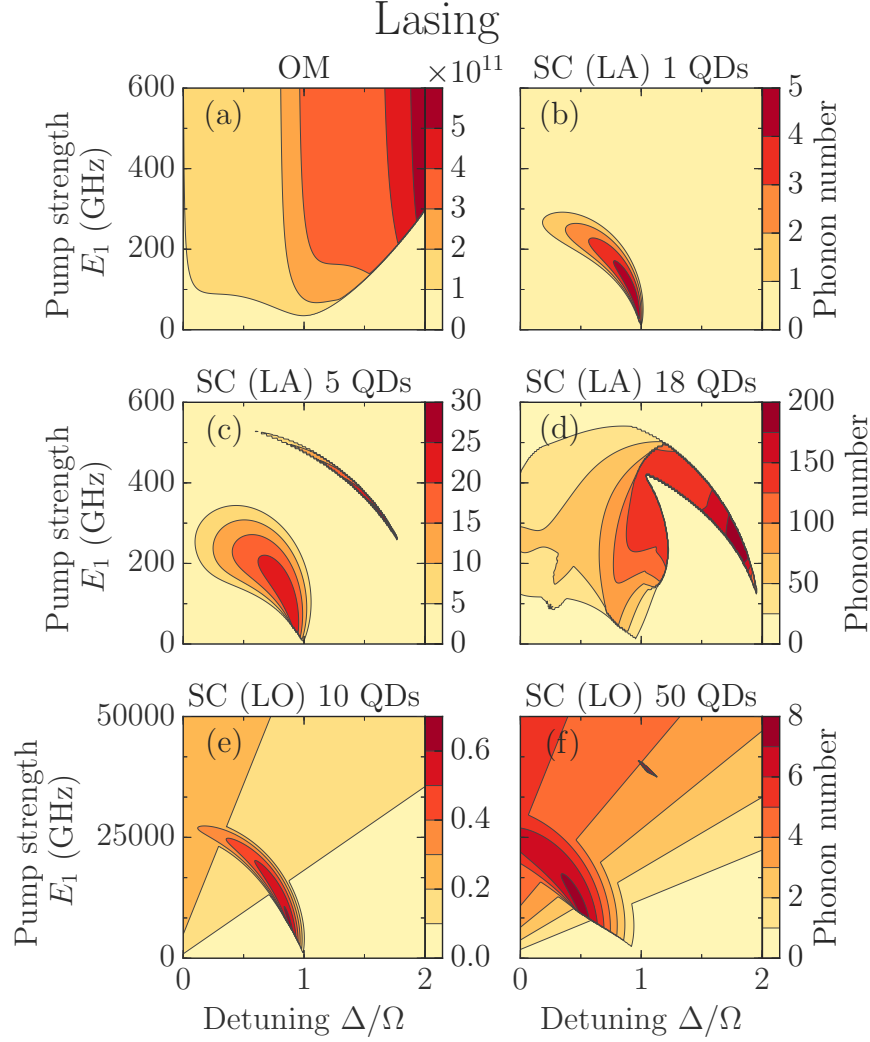


Figure 6. The mean phonon number is plotted as a function of the pump strength and the detuning for the OM system (a), the SC (LA) system with 1 (b), 5 (c), and 18 (d) QDs, and the SC (LO) system with 10 (e) and 50 (f) QDs.

For the OM system, the effective detuning is $\Delta_{\text{eff}} = -\Delta - \frac{g^2}{\Omega} n_{\text{HF}}$. This reveals, that there is no self-quenching, but also a dispersive shift, which is proportional to the number of photons in the cavity. This is analog to the proportionality to n_{HF} in the SC case. Due to the weak coupling strength for most OM systems, the dispersive shift becomes only important for very high pump strengths.

Further, for larger numbers of QDs [cf. Fig. 6(d)], the one and two phonon lines mix so that the maximum for phonon lasing not only involves a first, but also a second order phonon-

assisted process. Then the above approximation becomes invalid.

The behavior of the SC system with LO phonons is similar to the one with LA phonons, but with lower phonon numbers due to the inefficient creation of phonons discussed earlier [cf. Fig. 6(e),(f)]. Nonetheless, the phonon number is still approximately proportional to the number of QDs, so that higher phonon numbers can be achieved by increasing the number of QDs. The mean number of phonons excited by the second order process is in a similar order of magnitude as the number of phonons in the stationary state for direct excitation. As in the case of LA phonons, the polaron shift and the self-quenching can be observed as well.

V. ENHANCEMENT OF DAMPING

The last effect, we will consider is the enhancement of the damping of the LF component through the interaction with the HF component. This effect is closely related to the lasing, which we examined in the previous section. It is also the basic mechanism involved in optomechanical backaction cooling.^{21,26,27} For a full description of cooling, thermal fluctuations have to be taken into account, which will not be done in this manuscript. Here, we employ a simplified analysis and set the focus on the enhancement of the damping, which is usually treated in terms of a linear response analysis of the system of Eq. (5).^{1,21}

The effective damping rate of the LF component, which gives the time the system needs to return to its stationary state, can be altered by the interaction with the HF component. At first we will investigate the increase of the damping in the OM and the SC system by evaluating the largest Lyapunov exponent for the LF part of the linearized equations of motion, as computed for the stability analysis in Sec. III.²⁵ This enables us to determine the most persistent oscillations in the phononic subsystem.

In Figs. 7, the largest Lyapunov exponent $\kappa_{\text{eff,L}}$ is shown for the different systems as a function of the detuning Δ and the pump strength E_1 . Note, that for the cooling in the OM case different parameters than for the bistability in Sec. III are used. This is done, because the stationary states become unstable shortly after the bistability for the parameters in Sec. III and the enhancement of the damping for the stable states is rather small in this case. To avoid this, a set of parameters with weaker coupling is used [cf. Tab. II]. For the SC system it is possible to use the same parameters as in the case of the bistability, since the damping

Enhancement of damping

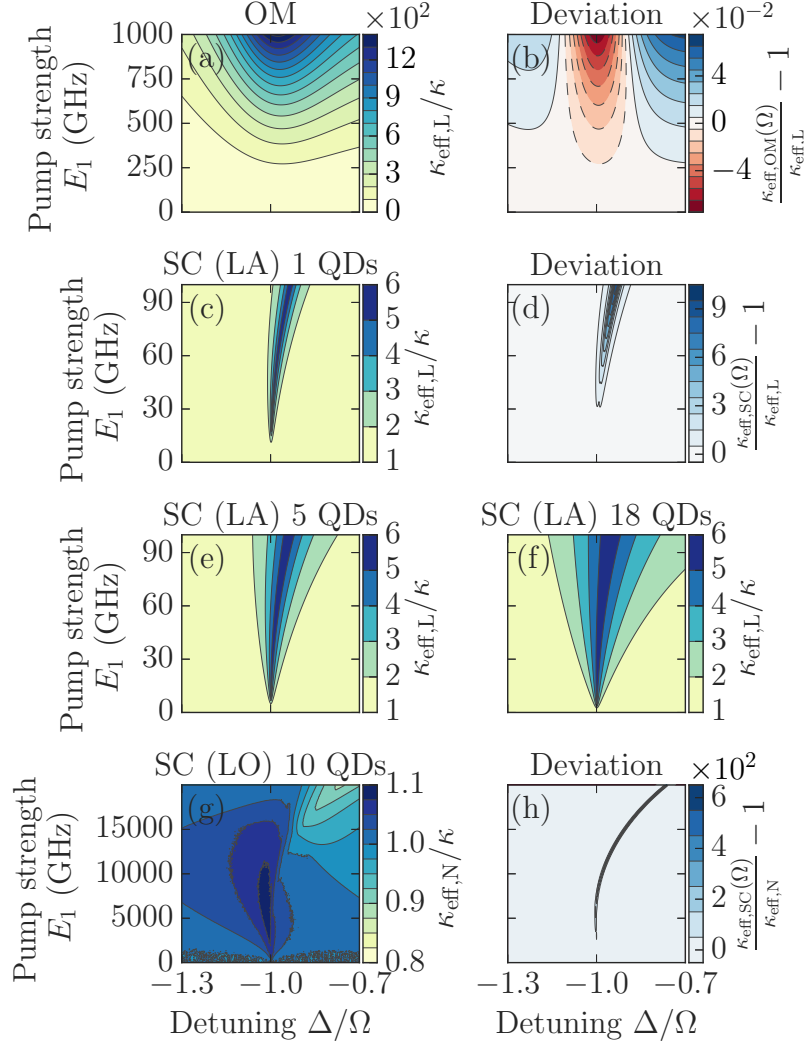


Figure 7. Here, the enhancement of the damping for the different systems as a function of pump strength and detuning is shown. (a) The damping in the OM system is enhanced by a factor of up to 1400 with the chosen parameters. (b) The analytical formula (9) is in good agreement in this case, since the deviation is only in the order of 10^{-2} . (c,e,f) For increasing numbers of QDs, the width of the enhancement of the damping increases, but it saturates at a factor of about 6. The analytical formula (d) predicts an enhancement with additional pump and with the number of QDs [cf. (10)]. For the SC system with LO phonons, the damping cannot be enhanced significantly (g). Even though the analytical formula only predicts a very high enhancement (h).

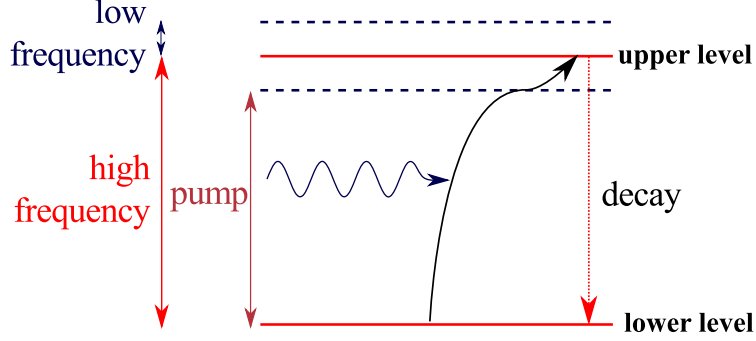


Figure 8. Scheme of the mechanism leading to enhanced damping. See text for explanation.

saturates before the relevant stationary state becomes unstable.

For the OM case [cf. Fig. 7(a)], we observe an enhancement of the damping with increasing pumping power up to a factor of 1400. In the SC case with LA phonons [cf. Fig. 7(c,e,f)], the damping is also enhanced but only by a factor of about six. This is to be expected, as the cooling utilizes the process complementary to lasing [cf. Fig. 8]: When the HF component is pumped, due to the detuning in the order of the negative phonon frequency, a phonon is absorbed. This process can again only be as fast as the decay of the QD excitation, while this restriction is not present in the OM case. In contrast to the lasing case, where more QDs could increase the maximal number of phonons, the damping cannot be increased by adding additional QDs. This is due to the fact, that the stationary phonon number is rather small in case of the SC systems (< 1). This way not enough phonons are present in the system, to make use of the mechanism depicted in Fig. 8 with multiple phonons simultaneously.

In the SC case with LO phonons, the damping cannot be computed via the largest Lyapunov exponent, since the phonon damping is not the slowest decay in this case [cf. Tab. II]. Here, we evaluate the damping numerically by fitting an exponential envelope to the time evolution of the phonon position. The damping determined this way is called $\kappa_{\text{eff},N}$. Fig. 7(g) shows the damping in the SC system for 10 QDs. The enhancement is so small, since the decay of the QD excitation is the same as in the LA case, while the phonon damping itself is already very high. Thus, the relevant process can only influence the damping marginally.

For small coupling strengths or pump rates, an analytical formula for the effective damping can be derived, as the dynamics in vicinity of the steady state is that of an effective damped oscillator without any interactions: $\dot{B}_{\text{eff}} = -(i\Omega_{\text{eff}} + \kappa_{\text{eff}})B$. Here, we also included an effective frequency Ω_{eff} , since the coupling in principle also changes the oscillation

frequency. For the parameters used in our cases, however, the effective frequency can be approximated by Ω . Note, that the effective treatment is only valid when the dynamics in vicinity of the steady state can be described by a damped harmonic oscillator. In general more complex dynamics are possible so that the analytical formula loses its validity.

To derive the formula, an external force acting on the LF component is taken into account in the Eqs. (5). This force could be a stochastic force originating from thermal fluctuations, which is needed for the analysis of cooling. The resulting equations are linearized in vicinity of the equilibrium positions and the result is Fourier transformed. From the resulting set of linear equations a susceptibility as the linear response to the external force can be computed. This is then compared to the susceptibility of a harmonic oscillator to incorporate the effects of the HF component on the LF component in the form of the frequency and the damping rate of an effective damped oscillator. More details on the calculations and all definitions are given in the App. C. For the OM system, the effective damping rate is²¹

$$\kappa_{\text{eff,OM}}(\bar{\omega}) = \kappa - \frac{4g^2 C_s^* C_s \Omega \gamma \tilde{\Delta}}{\left[\gamma^2 + (\bar{\omega} + \tilde{\Delta})^2 \right] \left[\gamma^2 + (\bar{\omega} - \tilde{\Delta})^2 \right]}, \quad (9)$$

which is valid for $C^* C \gg 1$. The formula for the SC case reads

$$\begin{aligned} \kappa_{\text{eff,SC}}(\bar{\omega}) = \kappa - \frac{2Ng^2 E_1 \Omega}{\bar{\omega}^2 + 4\gamma^2} & \\ & \left\{ \left[\text{Re}(P_s) \tilde{\Delta} - \text{Im}(P_s) (\gamma - \gamma_{\text{PD}}) \right] \left(\gamma_r^2 - \tilde{\Delta}^2 - \omega_R^2 \right) \right. \\ & \left. + 2 \left[2\text{Re}(P_s) \tilde{\Delta} \gamma + \text{Im}(P_s) (2\gamma \tilde{\gamma} + \bar{\omega}^2) \right] \gamma_r \sqrt{1 + \frac{\mathcal{D}}{2}} \sqrt{1 - \frac{4E_1^2}{\bar{\omega}^2 + 4\gamma^2}} \right\} \\ & / \left\{ \left[\gamma_r^2 + (\omega_R + \tilde{\Delta})^2 \right] \left[\gamma_r^2 + (\omega_R - \tilde{\Delta})^2 \right] + 2\mathcal{D} \gamma_r^2 \omega_R^2 \right\} \quad (10) \end{aligned}$$

and is valid for weak excitation.

In both cases $\tilde{\Delta} = \Delta + \frac{Ng^2 \Omega U_s}{\Omega^2 + \kappa^2}$. This includes the dispersive shift in case of the stationary state. This reveals why the dispersive shift is only observed in the OM system: The dispersive shift is proportional to the stationary number of excitations in the system, which is small for the SC system, while it is significant in the OM case. Even though the formula for the SC case is more complicated some similarities can be observed. In case of weak excitation the formula can be simplified by approximating $\omega_R \approx \omega$, $\gamma_r \approx \tilde{\gamma}$, and $\mathcal{D} \approx 0$. The major

restriction of the analytical formula is, that it relies on harmonic dynamics. For both systems this approximation fails at some point, but since the coupling in the OM system is weaker, the region of validity is very large and the deviation is only small. This is shown in Fig. 7(b) for the OM and in Fig. 7(d) for the SC system. The deviation of the analytical formula from the full computation is given: For the OM case, only a small differences in the order of a few percent are observed [cf. Fig. 7(b)], while for the SC systems, the formula overestimates the effect of cooling drastically, especially for large pump powers [cf. Figs. 7(f,h)].

VI. CONCLUSION

In conclusion, we studied similarities in the behavior of an optomechanical and a semiconductor system with a single phonon mode, constituted by either a single acoustic phonon mode or an effective optical phonon mode. We showed that the mechanical mode of the mirror has the same function as the phonon mode. Also, the cavity resonance and the optical resonance of the quantum dot are analogous. The underlying model is a Hamiltonian formulation, from which equations of motion are derived.

Even though the systems exhibit similar features, the underlying physics are different. In particular, as already discussed in the model section II, the high frequency component is bosonic in the optomechanical case, while it is fermionic in the semiconductor case.

Both systems exhibit the nonlinear effect of bistability. Here, the optomechanical system can be understood as the limit of the semiconductor system with many quantum dots. This is the case, since the additional equation, needed for the description of the fermionic quantum dots, is not necessary for weak excitation of the quantum dots.

Furthermore, the detuning of the system resonance from the pump laser can be used to control the behavior of the phonon mode: In the blue-detuned regime, the number of phonons is strongly increased, leading to phonon lasing. In the red-detuned regime, the damping of the phonon mode is enhanced.

In case of phonon lasing, the number of coherent phonons is very large for the optomechanical system since the relevant processes are not limited strictly by the lifetime of the high frequency component. For the semiconductor system, this limitation is given, since the quantum dot can only be excited again after its excitation has decayed. The phonon number can be increased by additional quantum dots coupled to the phonon mode for the

semiconductor system. In case of optical phonons, however, their short lifetimes prevent a significant occupation of the phonon mode.

The damping may be enhanced for the optomechanical system and the semiconductor system with acoustic phonons. For optical phonons an enhancement of the damping cannot be observed. This is attributed to the choice of parameters, especially to the short phonon lifetime. For the optomechanical system, the damping may be increased strongly before other effects dominate and prevent an enhancement. For the semiconductor system, the damping may only be enhanced weakly. Even additional quantum dots do not allow a further enhancement, which would be suggested from the observations for lasing.

ACKNOWLEDGMENTS

We are grateful towards the Deutsche Forschungsgemeinschaft for support through SFB 910 and SFB 787 as well as the Sandia LDRD program, funded by the U.S. Department of Energy under Contract No. DE-AC04-94AL85000.

Appendix A: Limiting behavior of the bistability

In case of the bistability [cf. Sec. III] the necessity for an equilibrium of forces $F_h + F_c = 0$ leads to a cubic equation with up to three real roots in the bistable regime. When using the relation $q_s = -\frac{\sqrt{2}g\Omega U_{\text{tot}}}{\Omega^2 + \kappa^2}$, which follows from (5a) in the stationary limit, the cubic equation can be expressed in terms of the excitation of the HF component. Note, that $U_{\text{tot}} = P^*P$ in the OM case and $U_{\text{tot}} = NU$ in the SC case. For the OM system, the equation, which has to be solved reads

$$\left[\left(\Delta + \frac{2g^2\Omega U_{\text{tot}}}{\Omega^2 + \kappa^2} \right)^2 + (\gamma + \gamma_{\text{PD}})^2 \right] U_{\text{tot}} = E_1^2. \quad (\text{A1})$$

The corresponding equation for the SC system reads

$$\left[\left(\Delta + \frac{2g^2\Omega U_{\text{tot}}}{\Omega^2 + \kappa^2} \right)^2 + (\gamma + \gamma_{\text{PD}})^2 \right] U_{\text{tot}} = NE_1^2 \left(1 - \frac{\gamma_{\text{PD}}}{\gamma} \right) \left(1 - 2\frac{U_{\text{tot}}}{N} \right). \quad (\text{A2})$$

If we neglect pure dephasing and assume $\frac{U_{\text{tot}}}{N} \ll 1$, i.e. a single QD is only excited weakly, the rule discussed in Sec. III for connecting the systems can be observed by comparing Eqs. (A1) and (A2).

Appendix B: Effective system

To gain further insight into the processes, which are relevant for lasing, an effective Hamiltonian is derived¹⁷. This takes only the second order process discussed in Sec. IV into account [cf. Fig. 4].

This is done in two steps: At first, a unitary transformation is applied in order to transform the Hamiltonian into a rotating frame. Afterwards, another unitary transformation is used to eliminate interactions in first order. The rotating frame is introduced by

$$\begin{aligned} H_{\text{RF}} &= U H U^\dagger - i \hbar U \partial_t U^\dagger, \\ U &= e^{\frac{i}{\hbar} \xi t}, \\ \xi &= \hbar \omega_L \hat{\mathbf{p}}^\dagger \hat{\mathbf{p}}. \end{aligned} \quad (\text{B1})$$

This leads to the Hamiltonian

$$H_{\text{RF}} = \underbrace{\hbar \Omega \hat{b}^\dagger \hat{b} - \hbar \Delta \hat{\mathbf{p}}^\dagger \hat{\mathbf{p}}}_{=H_0} + \underbrace{\hbar g \hat{\mathbf{p}}^\dagger \hat{\mathbf{p}} (\hat{b} + \hat{b}^\dagger)}_{=H_1} + i \hbar \mathbf{E} (\hat{\mathbf{p}}^\dagger - \hat{\mathbf{p}}), \quad (\text{B2})$$

where, as above, $\Delta = \omega_L - \omega$. This way, the explicit time dependence of the Hamiltonian is eliminated. In the next step, the unitary transformation

$$H_{\text{eff}} = e^{iS} H e^{-iS} \approx H_0 + H_1 + [iS, H_0 + H_1] + \frac{1}{2}[iS, [iS, H_0]] \quad (\text{B3})$$

is applied such that only interaction terms of second order are present. By choosing $S = \alpha \hat{\mathbf{p}} + \beta \hat{\mathbf{p}}^\dagger \hat{\mathbf{p}} + H.c.$, the first order terms can be eliminated, and the effective Hamiltonian can be computed from

$$H_{\text{eff}} = H_0 + \frac{1}{2}[iS, H_1]. \quad (\text{B4})$$

This is achieved with $\alpha = -\frac{\mathbf{E}}{\Delta}$ and $\beta = i\frac{g}{\Omega}$. The effective Hamiltonian reads then

$$\begin{aligned} H_{\text{eff}} &= \hbar \Omega \hat{b}^\dagger \hat{b} - \hbar \Delta \hat{\mathbf{p}}^\dagger \hat{\mathbf{p}} + \frac{\hbar}{\Delta} W - \hbar \frac{g^2}{\Omega} \hat{\mathbf{p}}^\dagger \hat{\mathbf{p}} \hat{\mathbf{p}}^\dagger \hat{\mathbf{p}} \\ &\quad + i \hbar \frac{g \mathbf{E}}{2} \left(\frac{1}{\Delta} + \frac{1}{\Omega} \right) (\hat{\mathbf{p}}^\dagger \hat{b}^\dagger - \hat{\mathbf{p}} \hat{b}) \\ &\quad + i \hbar \frac{g \mathbf{E}}{2} \left(\frac{1}{\Delta} - \frac{1}{\Omega} \right) (\hat{\mathbf{p}}^\dagger \hat{b} - \hat{\mathbf{p}} \hat{b}^\dagger). \end{aligned} \quad (\text{B5})$$

Here, we shifted the energy scale appropriately. The first two terms are the energy of the LF component and of the HF component in the rotating frame. The third term can

be neglected in the OM case, where it constitutes a shift of the total energy scale of the Hamiltonian ($W_{\text{OM}} = \mathbf{E}^2$). In the SC case, this term introduces the self-quenching and can be written as $W_{\text{SC}} = 2 \sum_{i=1}^{N_{\text{QD}}} E_i^2 \hat{p}_i^\dagger \hat{p}_i$. The fourth term describes the dispersive shift. It depends on the number of excitations in the system. The fifth term models two processes, which are energy conserving in the case of lasing [cf. Fig. 4]: The number of excitations in the HF component is increased (decreased) by the external field and a phonon is emitted (absorbed). The last term describes processes, which are energy conserving in case of cooling [cf. Fig. 8]: The number of excitations in the HF component is increased (decreased) by the external field and a phonon is absorbed (emitted). Depending on the scenario one of the two terms can be neglected.

Appendix C: Effective damping analytical

The formulas for the effective damping are derived in analogy to Ref.²¹, while we use the semiclassical equations as starting point. For the linearized system, this leads to the same susceptibility¹. At first the system of equations (5) is linearized in vicinity of the steady state. In addition an external force F on the LF component is taken into account: $\dot{B} = -(i\Omega + \kappa)B - iNgU + iF/\sqrt{2}$. Then, the real variables $q = \frac{B+B^*}{\sqrt{2}}$, $p = \frac{B-B^*}{\sqrt{2}i}$, $X = \frac{P+P^*}{\sqrt{2}}$, and $Y = \frac{P-P^*}{\sqrt{2}i}$ are introduced and the the deviation from the steady state is defined as $\delta q(t) = q(t) - q_s$. Here, the index s indicates the stationary value. When terms, which are nonlinear in the deviations, are neglected, a set of linear differential equations emerges. This can be Fourier transformed, leading to the sets of equations

$$-i\bar{\omega}\mathcal{F}_q = \Omega\mathcal{F}_p - \kappa\mathcal{F}_q \quad (\text{C1a})$$

$$-i\bar{\omega}\mathcal{F}_p = -\Omega\mathcal{F}_q - \kappa\mathcal{F}_p - g_X\mathcal{F}_X - g_Y\mathcal{F}_Y + \mathcal{F}_F \quad (\text{C1b})$$

$$-i\bar{\omega}\mathcal{F}_X = \tilde{\Delta}\mathcal{F}_Y - \gamma\mathcal{F}_X + g_Y\mathcal{F}_q \quad (\text{C1c})$$

$$-i\bar{\omega}\mathcal{F}_Y = -\tilde{\Delta}\mathcal{F}_X - \gamma\mathcal{F}_Y - g_X\mathcal{F}_q \quad (\text{C1d})$$

for the OM system and

$$-i\bar{\omega}\mathcal{F}_q = \Omega\mathcal{F}_p - \kappa\mathcal{F}_q \quad (\text{C2a})$$

$$-i\bar{\omega}\mathcal{F}_p = -\Omega\mathcal{F}_q - \kappa\mathcal{F}_p - \sqrt{2}Ng\mathcal{F}_U + \mathcal{F}_F \quad (\text{C2b})$$

$$-i\bar{\omega}\mathcal{F}_X = \tilde{\Delta}\mathcal{F}_Y - \tilde{\gamma}\mathcal{F}_X + g_Y\mathcal{F}_q - 2\sqrt{2}E_1\mathcal{F}_U \quad (\text{C2c})$$

$$-i\bar{\omega}\mathcal{F}_Y = -\tilde{\Delta}\mathcal{F}_X - \tilde{\gamma}\mathcal{F}_Y - g_X\mathcal{F}_q \quad (\text{C2d})$$

$$-i\bar{\omega}\mathcal{F}_U = \sqrt{2}E_1\mathcal{F}_X - 2\mathcal{F}_U \quad (\text{C2e})$$

for the SC system. The \mathcal{F} indicates the Fourier transform of the respective variable. The Fourier transforms are always functions of $\bar{\omega}$. We introduced the definitions $\tilde{\gamma} = (\gamma + \gamma_{\text{PD}})$, $\tilde{\Delta} = \Delta + \sqrt{2}gq_s$, $g_X = \sqrt{2}gX_s$, and $g_Y = \sqrt{2}gY_s$.

This system of equations can be solved so that, the susceptibility as the linear response to the external force can be computed from $\mathcal{F}_q = \chi(\bar{\omega})\mathcal{F}_F$. In the case of the OM system, the inverse of the susceptibility reads

$$\chi_{\text{OM}}^{-1}(\bar{\omega}) = -\frac{\bar{\omega}^2 + 2i\bar{\omega}\kappa - \kappa^2 + \Omega^2}{\Omega} - \frac{2g^2P_s^*P_s\tilde{\Delta}}{(\gamma - i\bar{\omega})^2 + \tilde{\Delta}^2}. \quad (\text{C3})$$

For the SC system, it is

$$\chi_{\text{SC}}^{-1}(\bar{\omega}) = -\frac{\bar{\omega}^2 + 2i\bar{\omega}\kappa - \kappa^2 + \Omega^2}{\Omega} + \frac{2gE_1N}{i\bar{\omega} - 2\gamma} \frac{g_X\tilde{\Delta} + g_Y(i\bar{\omega} - \tilde{\gamma})}{(-i\omega(1-R) + \tilde{\gamma} + 2R\gamma)(\tilde{\gamma} - i\bar{\omega}) + \tilde{\Delta}^2}. \quad (\text{C4})$$

Here, we introduced the definition $R = \frac{4E_1^2}{\bar{\omega}^2 + 4\gamma^2}$. Differences to Ref.²¹ for the OM system arise from differences in the definition of the parameters [cf. Tabs. I, II] and the introduction of damping. In the limit $\Omega \gg \kappa$, which is valid for the systems we are interested in, both descriptions are equivalent. From the susceptibilities, the effective dampings (9) and (10) can be computed, where we use

$$\mathcal{D} = \frac{1}{2} \frac{R^2 \left(1 - \frac{2\gamma}{\tilde{\gamma}}\right)^2}{1 - \left(1 + \frac{2\gamma}{\tilde{\gamma}}\right) R + \frac{2\gamma}{\tilde{\gamma}} R^2}$$

$$\gamma_r = \tilde{\gamma} \sqrt{1 - \frac{2\gamma}{\tilde{\gamma}} R}$$

$$\omega_R = \bar{\omega} \sqrt{1 + R}.$$

Table I. Parameter values for the bistabilities in Sec. III.

	Optomechanical ²⁴	Semiconductor (LA) ¹⁷	Semiconductor (LO)
Detuning of pump and	$\Delta = -2.6 \times \Omega$	$\Delta = -\Omega/8$	$\Delta = -\Omega$
LF component	$\Omega = 2\pi \times 10$ MHz	$\Omega = 556.6$ GHz	$\Omega = 55.3$ THz
Losses	opt. cavity $\gamma = 2\pi \times 14$ MHz	TLS $\gamma = 5$ GHz	$\gamma = 5$ GHz
	mech. resonator $\kappa = 2\pi \times 50$ Hz	acoust. cav. $\kappa = 0.5$ GHz	$\kappa = 100$ GHz
			$\gamma_{\text{PD}} = 100$ GHz ²⁸
coupling strength	$ g = 952.7$ Hz	$ g = 197.5$ GHz	$ g = 5.1$ THz
Number of QDs	–	1	10

Appendix D: Parameters

-
- ¹ M. Aspelmeyer, T. J. Kippenberg, and F. Marquardt, *Rev. Mod. Phys.* **86**, 1391 (2014).
- ² T. J. Kippenberg and K. J. Vahala, *Science* **321**, 1172 (2008).
- ³ C. M. Caves, *Phys. Rev. Lett.* **45**, 75 (1980).
- ⁴ K. Zhang, F. Bariani, and P. Meystre, *Phys. Rev. Lett.* **112**, 150602 (2014).
- ⁵ X. B. Zhang, T. Taliercio, S. Kolliakos, and P. Lefebvre, *Journal of Physics: Condensed Matter* **13**, 7053 (2001).
- ⁶ M. D. Eisaman, J. Fan, A. Migdall, and S. V. Polyakov, *Review of Scientific Instruments* **82**, 071101 (2011).
- ⁷ J. Restrepo, C. Ciuti, and I. Favero, *Phys. Rev. Lett.* **112**, 013601 (2014).
- ⁸ A. Carmele, J. Kabuss, and W. W. Chow, *Phys. Rev. B* **87**, 041305 (2013).
- ⁹ N. D. Lanzillotti-Kimura, A. Fainstein, C. A. Balseiro, and B. Jusserand, *Phys. Rev. B* **75**, 024301 (2007).
- ¹⁰ Ö. O. Soykal, R. Ruskov, and C. Tahan, *Phys. Rev. Lett.* **107**, 235502 (2011).
- ¹¹ M. Trigo, A. Bruchhausen, A. Fainstein, B. Jusserand, and V. Thierry-Mieg, *Phys. Rev. Lett.* **89**, 227402 (2002).
- ¹² G. Rozas, M. F. Pascual Winter, B. Jusserand, A. Fainstein, B. Perrin, E. Semenova, and A. Lemaître, *Phys. Rev. Lett.* **102**, 015502 (2009).

- ¹³ A. Fainstein, N. D. Lanzillotti-Kimura, B. Jusserand, and B. Perrin, *Phys. Rev. Lett.* **110**, 037403 (2013).
- ¹⁴ N. Lanzillotti-Kimura, A. Fainstein, and B. Jusserand, *Ultrasonics* **56**, 80 (2015).
- ¹⁵ E. A. Muljarov and R. Zimmermann, *Phys. Rev. Lett.* **98**, 187401 (2007).
- ¹⁶ J. Kabuss, A. Carmele, M. Richter, and A. Knorr, *Phys. Rev. B* **84**, 125324 (2011).
- ¹⁷ J. Kabuss, A. Carmele, T. Brandes, and A. Knorr, *Phys. Rev. Lett.* **109**, 054301 (2012);
J. Kabuss, A. Carmele, and A. Knorr, *Phys. Rev. B* **88**, 064305 (2013).
- ¹⁸ F. Marquardt, J. G. E. Harris, and S. M. Girvin, *Phys. Rev. Lett.* **96**, 103901 (2006).
- ¹⁹ M. Ludwig, B. Kubala, and F. Marquardt, *New Journal of Physics* **10**, 095013 (2008).
- ²⁰ J. Chan, T. P. M. Alegre, A. H. Safavi-Naeini, J. T. Hill, A. Krause, S. Gröblacher, M. Aspelmeyer, and O. Painter, *Nature* **478**, 89 (2011).
- ²¹ C. Genes, D. Vitali, P. Tombesi, S. Gigan, and M. Aspelmeyer, *Phys. Rev. A* **77**, 033804 (2008).
- ²² C. K. Law, *Phys. Rev. A* **51**, 2537 (1995).
- ²³ T. Holstein and H. Primakoff, *Phys. Rev.* **58**, 1098 (1940).
- ²⁴ R. Ghobadi, A. R. Bahrapour, and C. Simon, *Phys. Rev. A* **84**, 033846 (2011).
- ²⁵ N. L. Naumann, S. M. Hein, A. Knorr, and J. Kabuss, *Phys. Rev. A* **90**, 043835 (2014).
- ²⁶ I. Wilson-Rae, N. Nooshi, W. Zwerger, and T. J. Kippenberg, *Phys. Rev. Lett.* **99**, 093901 (2007).
- ²⁷ F. Marquardt, J. P. Chen, A. A. Clerk, and S. M. Girvin, *Phys. Rev. Lett.* **99**, 093902 (2007).
- ²⁸ P. Machnikowski, *Phys. Rev. Lett.* **96**, 140405 (2006).

Table II. Parameter values for enhancing or decreasing the damping used throughout Secs. IV and V.

	Optomechanical ²¹	Semiconductor ¹⁷	Semiconductor (LO)
pump rate	$E_1 = 60$ GHz [cf. Fig. 5(a)]	$E_1 = 80$ GHz [cf. Fig. 5(b)]	$E_1 = 9.01$ THz [cf. Fig. 5(c)]
Detuning of pump (+: Lasing, -: enhancement of damping)	$\Delta \approx \pm\Omega$	$\Delta \approx \pm\Omega$	$\Delta \approx \pm\Omega$
LF component	$\Omega = 2\pi \times 10$ MHz	$\Omega = 556.6$ GHz	$\Omega = 55.3$ THz
Losses	opt. cavity $\gamma = 2\pi \times 2$ MHz	TLS $\gamma = 5$ GHz	$\gamma = 5$ GHz $\gamma_{\text{PD}} = 100$ GHz
	mech. resonator $\kappa_{\text{m}} = 2\pi \times 50$ Hz	acoust. cav. $\kappa = 0.5$ GHz	$\kappa = 50$ GHz
coupling strength	$ g = 205$ Hz	$ g = 197.5$ GHz	$ g = 5.1$ THz
Number of QDs	–	1 [cf. Fig. 5(b)], 5, 18	10 [cf. Fig. 5(c)], 50